Quantum Electronics **46** (9) 795–800 (2016)

CONTROL OF LASER RADIATION PARAMETERS DOI: 10.1070/QEL16085

Performance characteristics and output power stability of a multichannel fibre laser

A.I. Kuzmenkov, S.N. Lukinykh, O.E. Nanii, A.I. Odintsov, A.P. Smirnov, A.I. Fedoseev, V.N. Treshchikov

Abstract. **The effect of the density and number of spectral channels on the output power stability in a multichannel cw laser has been studied theoretically and experimentally. In our calculations, we used a model in which the interaction between channels due to gain medium saturation was determined by channel frequency spacing-dependent cross-saturation coefficients. The key features of lasing have been analysed and illustrated by the examples of three-, five- and nine-channel lasers. It has been shown that, at a given excess of the pump power over threshold, the channel powers can be equalised by introducing additional losses into the highest power channels. At a sufficiently high channel density, raising the pump power then leads to termination of lasing in the even channels. As the number of channels increases, the laser system retains its stability, but the time needed for the transition to a steady state increases sharply. In our experiments, we used an erbium-doped fibre laser whose design ensured independent control over the powers of up to 40 spectral channels anchored on the telecommunication frequency grid. Our experimental data are in qualitative agreement with the calculation results. In particular, a long-term relative instability less than 3 dB was only observed at a number of channels less than seven and channel frequency spacings above 400 GHz. Instability was shown to increase with an increase in the number and density of channels.**

Keywords: *multichannel laser, erbium-doped fibre laser, wavelength-division multiplexing, multichannel communication systems, telecommunication frequency grid.*

1. Introduction

Multichannel lasers have a number of advantages over single-frequency lasers when used in interferometry, range finding, holography, rf photonics and environmental monitoring owing to the possibility of employing differential measurement techniques. Multichannel lasers can be used to make highly sensitive, precision optical devices and systems [1–7]. Studies of the performance characteristics of such lasers were typically limited to two or four channels [8–13].

A very important application area of multichannel lasers with a large number of channels is optical fibre communication, where such lasers are employed as multichannel transmitters in a new generation of communication systems. In particular, modern multichannel, wavelength-division multiplexing communication systems have up to 80 channels operating in the spectral band of erbium-doped fibre amplifiers at a standard channel frequency spacing of 50 GHz. The overall transmission capacity of the communication systems reaches 8 Tbit s^{-1} [14–22].

To design and test multiterabit communication systems, a multichannel light source (having 40 to 96 channels) is needed, with the possibility of tuning the wavelengths of its channels over the range 1530–1560 nm. Such a laser was proposed by Popov et al. [23], but only two- and three-channel lasing was achieved in experiments.

Multichannel lasing with more than ten channels was first demonstrated by Park and Wysocki [24], with erbium-doped fibre cooled to liquid nitrogen temperature. Clearly, such a configuration is of little utility for practical application in communication systems. In the last decade, a variety of multichannel fibre lasers have been proposed and demonstrated [25–31], in which channel powers are equalised using various combinations of modulators and nonlinear optical and active elements located in controlled-anisotropy cavities of complex design.

In particular, to stabilise multichannel lasing, additional fibres, in which stimulated Raman or Brillouin scattering conditions were ensured, were introduced into an erbium-doped fibre laser [25, 26], or an intracavity semiconductor amplifier was used [27]. For this purpose, use was also made of different intracavity nonlinear optical effects [28–31]: intracavity polarisation rotation [28, 29] and a nonlinear fibre loop mirror [30, 31]. Note that Liu et al. [31] incorporated an active element into the nonlinear mirror. According to Zhang et al. [28], Feng et al. [29, 30] and Liu et al. [31], basic to the multichannel lasing stabilisation principle is the choice of the operating point of nonlinear elements where they will stabilise the output power at some fixed level.

However, none of the mentioned studies addressed the nature of the competitive interaction between spectral channels in an active element, and the principles of multichannel lasing stabilisation in nonlinear devices were described in those studies only qualitatively, without sufficient clarity, which makes it impossible to utilise them for further optimisation of laser operation conditions. From the viewpoint of practical application, a serious drawback to most of the multichannel

A.I. Kuzmenkov, A.I. Odintsov, A.I. Fedoseev Faculty of Physics, M.V. Lomonosov Moscow State University, Vorob'evy gory, 119991 Moscow, Russia;
S.N. Lukinykh, O.E. Nanii Faculty of Physics, M.V. Lomonosov Moscow State University, Vorob'evy gory, 119991 Moscow, Russia; T8 LLC, Krasnobogatyrskaya ul. 44/1, 107076 Moscow, Russia; e-mail: naniy@t8.ru;
A.P. Smirnov Faculty of Computational Mathematics and Cybernetics, M.V. Lomonosov Moscow State University, Vorob'evy gory, 119991 Moscow, Russia;
V.N. Treshchikov T8 LLC, Krasnobogatyrskaya ul. 44/1, 107076 Moscow, Russia

Received 23 March 2016; revision received 4 August 2016
Kvantovaya Elektronika **46** (9) 795–800 (2016)
Translated by O.M. Tsarev

lasers studied to date is that their parameters should be adjusted to a given operation mode, in particular, that polarisers should be adjusted manually in line with changes in the gain coefficient of the active fibre. However, the main drawback of the above nonlinear methods for multichannel lasing stabilisation is the possibility of switching from the multichannel lasing stabilisation regime to passive mode locking (see e.g. Ref. [31]).

In this work, we examine the effect of the density and number of spectral channels on the performance characteristics and output power stability of a multichannel cw erbium-doped fibre laser. Our experimental equipment allows us to study lasing for up to 40 channels. The key features of steady-state, controlled-loss lasing are illustrated by the examples of three-, five- and nine-channel lasers. Calculation results indicate that the numerical model used provides an adequate qualitative description of the experimental data for up to ten channels. We obtained good quantitative agreement of results for three channels and satisfactory agreement for five channels.

2. Calculational model

The calculational model builds on balance equations. Individual lasing channels interact through inversion cross saturation. In this approximation, the equations for the power p_i and gain coefficient g_i of each channel ($i = 1, 2, ..., N$) in terms of normalised quantities have the form [32]

$$\frac{dp_i}{d\tau} = [(g_i - 1 - \delta_i)p_i]\mu, \tag{1}$$

$$\frac{dg_i}{d\tau} = q - g_i\left(1 + p_i + \sum_{i\neq j}^{N}\zeta_{ij}p_j\right), \tag{2}$$

where $\tau = t/T_1$; t is time; T_1 is the inverted population relaxation time; $\mu = T_1/T_{ph}$; T_{ph} is the field attenuation time in the cavity; q is the pump power in excess of threshold, common to all the channels; δ_i is an additional loss in the channels; and ζ_{ij} are cross-saturation coefficients.

In calculations, we used cross-saturation coefficients similar to those determined experimentally by Popov et al. [23] from channel powers in a two-channel system as functions of the loss in one of the channels. In particular, we used a symmetric set of coefficients: $\zeta_{ij} = \zeta_{ji}$. The decrease in ζ_{ij} with increasing channel frequency spacing $\Delta\nu$ (from $\zeta_{ii} = 1$ at $\Delta\nu = 0$ to $\zeta_0 = 0.78$ at $\Delta\nu > 900$ GHz) was represented by either a Gaussian, $\zeta_{ij} = \zeta_0 + (1 - \zeta_0)\exp\{-[(j - i)/H]^2\}$, or Lorentzian, $\zeta_{ij} = \zeta_0 + (1 - \zeta_0)\{[(j - i)/H]^2 + 1\}^{-1}$, where $H = \Delta\nu_H/\Delta\nu$ and $\Delta\nu_H$ is the full width at half maximum (FWHM) of the spectral dip in the gain profile of the erbium-doped fibre laser (according to Popov et al. [23] and Bolshtyansky [33], $\Delta\nu_H = 450$ GHz). The calculations were made for H from 0.225 (channel spacing $\Delta\nu = 2000$ GHz) to 4.5 ($\Delta\nu = 100$ GHz). Our numerical calculation results indicate that the nature of the competition between the lasing channels in the multichannel lasing regime is influenced only slightly by the model shape of the dip (Gaussian or Lorentzian) but depends strongly on the ratio of the FWHM of the dip to the frequency spacing between the competing channels (parameter H) and on the cross-saturation coefficient at an asymptotically infinite frequency spacing between the competing channels (parameter ζ_0).

To model a configuration of practical importance in which all channels have identical powers ($p_i \equiv p$), we first calculated the additional loss δ_i in the channels at a given value of q. It follows from a steady-state solution to Eqn (2) that

$$\delta_i = \frac{q}{1 + pS_i} - 1, \tag{3}$$

where $S_i = \sum_{j=1}^{N}\zeta_{ij}$. Note that the sum is maximal for the central channel and minimal for the extreme channels. Assuming that $S_c = \sum_{j=1}^{N}\zeta_{cj}$ and $\delta_c = 0$ for the central channel and using (3), we obtain formulas for the steady-state power and the loss in each channel:

$$p = (q - 1)/S_c, \tag{4}$$

$$\delta_i = \frac{(q - 1)(S_c - S_i)}{S_c + (q - 1)S_i}. \tag{5}$$

According to (5), the added loss increases from zero in the central channel to a maximum level in the extreme channels.

3. Experimental

We experimentally studied a modular erbium-doped fibre laser which comprised an EDFA (Onega EA-16V/23 amplifier) and wavelength-selective switch (WSS) module, both available commercially for optical fibre communication systems. Figure 1 shows a schematic of the experimental setup. The active element used (*1*) is a 10-m length of erbium-doped fibre pumped at a wavelength $\lambda = 980$ nm by a semiconductor laser (*2*). The pump current can be tuned over the range 60–300 mA, which allows the unsaturated gain coefficient to be varied from 16 to 30 dB. Unidirectional lasing is ensured by built-in input and output optical isolators (*3*), which prevent amplification of reflected parasitic emission. A wavelength-selective coupler (*4*) launches pump light into the active fibre. A spectral selector (*5*) smooths the spectral inhomogeneity of the gain coefficient of the erbium-doped fibre. About 10% of the laser output is directed through a coupler (*6*) to the wavelength-selective switch (WSS module), which is included in the laser feedback loop. The transmission spectrum of this module corresponds to the telecommunication frequency grid, and each channel contains a separate computer-controlled attenuator with a dynamic attenuation tuning range of 30 dB and a step of 0.1 dB. Another coupler (*7*) sends 1% of the laser output to an Anritsu MS9710B spectrum analyser (*9*). In its operating wavelength range 600–1750 nm, its measurement accuracy is $\Delta\lambda \approx \pm 0.05$ nm at powers from –90 to +10 dBm.

Most of the laser light is directed to a power meter (*10*) through an OM-40-AV-PM demultiplexer (*8*), which couples

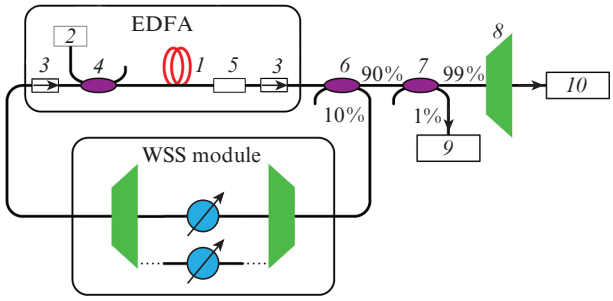

Figure 1. Schematic of the experimental setup:
(*1*) active element; (*2*) pump laser; (*3*) optical isolators; (*4*) wavelength-selective coupler; (*5*) spectral selector which smooths the difference in gain coefficient between the channels; (*6*) 10/90 coupler; (*7*) 1/99 coupler; (*8*) demultiplexer; (*9*) spectrum analyser; (*10*) power meter.

the light into different channels. The setup is controlled by a Dnepr control system through a standard web interface. The minimum total loss in the WSS module, couplers and patch cords is about 16 dB.

In our experiments, the lasing frequencies of the channels were determined by the transmission spectrum of the wavelength-selective switch (WSS) and, hence, corresponded to the telecommunication frequency grid. To ensure that a given number of channels had identical output powers, we used the following power equalisation procedure at a fixed pump current: Using the attenuators of the switch (*6*), we minimised the loss in all the channels. The additional loss in the highest power channel was increased in 0.1-dB increments until the power of this channel was lower than that of the second highest power channel. Next, the same was done for the other highest power channel. This procedure allowed us to equalise the powers of up to seven channels at a frequency spacing of 600 GHz ($H = 0.75$) or greater. The long-term relative power instability was then within 3 dB. Reducing the frequency spacing significantly increased the instability. In a nine-channel laser, we failed to achieve stable lasing with roughly equal channel powers even at a maximum channel frequency spacing of 500 GHz ($H = 0.9$): the minimum scatter in power was ~8 dB.

4. Results and discussion

4.1. Three-channel laser

Figure 2 shows calculated channel powers as functions of q at a varied channel density. The channels are identical in loss, and the effect of the cross-saturation mechanism is such that the power of the second (central) channel is always lower than that of the side channels. With increasing pump power, the channel powers increase linearly but with different slopes. For this reason, the sensitivity of each channel to changes in pump power can be characterised by the derivative $\eta_i = \mathrm{d}p_i/\mathrm{d}q$. The channel density, which is determined by the parameter H in the model under consideration, has a significant effect on the sensitivity of the channels. At a low channel density [Fig. 2, lines (*1*, *2*)], the sensitivities of all the channels, η_i, are essentially identical. With increasing channel density [lines (*1′*, *2′*)], the sensitivity of the side channels, $\eta_{1,3}$, increases, whereas that of the central channel, η_2, decreases. If the channel density ensures that the condition $2\zeta_{12} \geqslant 1 + \zeta_{13}$ is fulfilled, no lasing occurs in the second channel at any value of q. The condition $2\zeta_{12} \geqslant 1 + \zeta_{13}$ corresponds to channel densities with $H > 4.5$. Thus, at a sufficiently high channel density in the laser and identical losses in the channels, no three-channel lasing occurs.

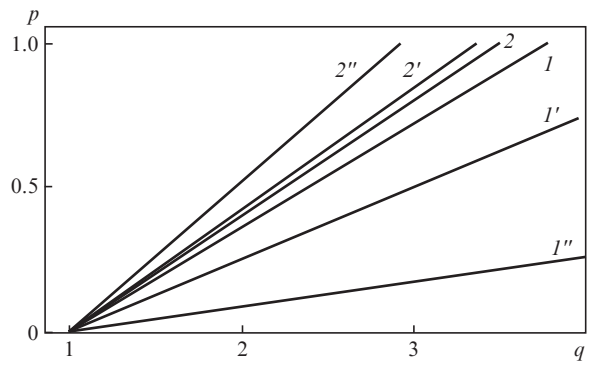

Figure 2. Output powers p of the (*1*, *1′*, *1″*) second channel and (*2*, *2′*, *2″*) two side channels vs. parameter q at identical losses in the channels and H = (*1*, *2*) 0.8, (*1′*, *2′*) 1 and (*1″*, *2″*) 3.

Experimentally, three-channel lasing with identical losses in the channels and roughly equal channel powers at a pump current $I_p = 200$ mA was achieved in the frequency range 400 GHz < $\Delta\nu$ < 2000 GHz, i.e. at a relatively low channel density. Increasing the channel density to a frequency spacing $\Delta\nu = 100$ GHz (corresponding to $H = 4.5$) leads to termination of lasing in the second channel.

Figure 3 illustrates the variation in channel powers with increasing pump power when the side channels have additional losses $\delta_1 = \delta_3 = 2.94 \times 10^{-2}$. It is seen in Fig. 3a that, at $H = 0.9$ ($\Delta\nu = 500$ GHz), the three channels have identical powers at $q = 3$. The parameter η_2 decreases sharply in response to the onset of lasing in the first and third channels. If the channel density is not very high, η_2 remains positive.

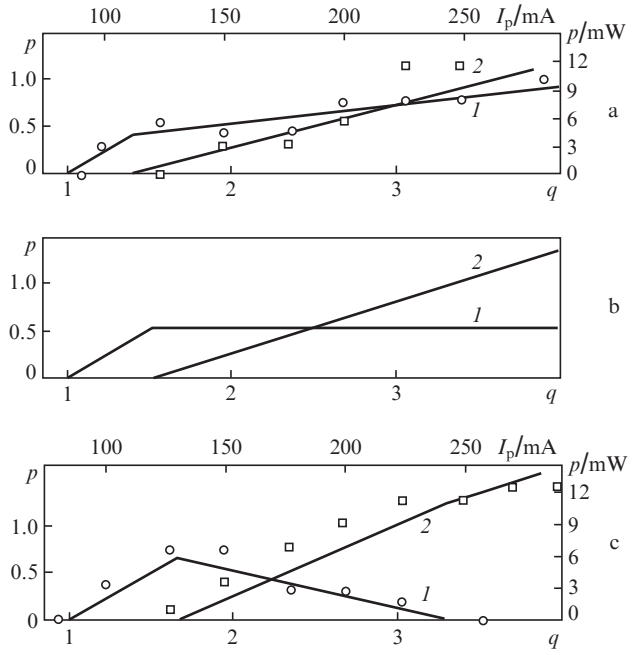

Figure 3. Calculated (solid lines) and measured (data points) output powers as functions of parameter q and pump current I_p for the (*1*, ○) second channel and (*2*, □) two side channels at H = (a) 0.9, (b) 1.45 and (c) 2, with additional losses in the side channels.

Increasing the channel density causes the second channel to lose its sensitivity to changes in pump power ($\eta_2 = 0$) at $H = 1.45$ (Fig. 3b). Further raising the channel density increases the competition between the channels to the extent that an increase in pump power leads to termination of lasing in the central channel ($\eta_2 < 0$). With increasing pump power ($q = 3.4$), the power of the second (central) channel drops to zero (Fig. 3c).

In our experiments, we achieved lasing at channel frequency spacings of 500 (calculation conditions corresponding to Fig. 3a) and 200 GHz (calculation conditions corresponding to Fig. 3c) and a lasing bandwidth of the channels under 0.05 nm (the resolving power of the spectrum analyser used). The lasing powers were equalised at a pump current I_p = 225 mA (Fig. 3a), and termination of lasing in the central

channel was observed at I_p = 260 mA (Fig. 3c). Under the conditions corresponding to Fig. 3b, we failed to achieve lasing in our experiments because we had no possibility to gradually vary the channel density (in our experiments, it was varied discretely, in 100-GHz increments).

Thus, lasing occurs in the second channel at a sufficient channel density and relatively low pump power, in the two side channels at high pump power and in the three channels at intermediate pump power.

4.2. Five-channel laser

Our calculations indicate that, at identical losses in all the channels, the behaviour of the channel powers in response to changes in pump power has the same general features as that in the three-channel laser. In experiments with identical losses in the channels, stable five-channel lasing occurs at not too high a channel density ($\Delta\nu > 500$ GHz). At $\Delta\nu < 400$ GHz, five-channel lasing is unstable: we observe a large scatter in channel power and large power fluctuations. At $\Delta\nu = 100$ GHz, the even channels are suppressed, and there is three-channel lasing with $\Delta\nu = 200$ GHz.

Figure 4 shows channel powers as functions of parameter q in the presence of additional losses $\delta_{1,5} = 1.34 \times 10^{-2}$, $\delta_{2,4} = 6.32 \times 10^{-4}$. Independent of channel density, the onset of lasing is observed at $q = 1$ in the central (third) channel, which has no additional loss. With increasing pump power, lasing begins in two more channels, depending on losses and $\Delta\nu$ (in the even channels in Fig. 4). In this process, η_3 changes sharply, remaining either positive or negative (Fig. 4, insets). In the latter case, lasing in the central channel terminates rather rapidly because of the relatively low additional losses in the even channels. In particular, in Figs 4a and 4b $p_3 = 0$ even at $q = 1.03$. Further raising the pump power produces the largest changes in the even channels, which are influenced by the two neighbouring channels.

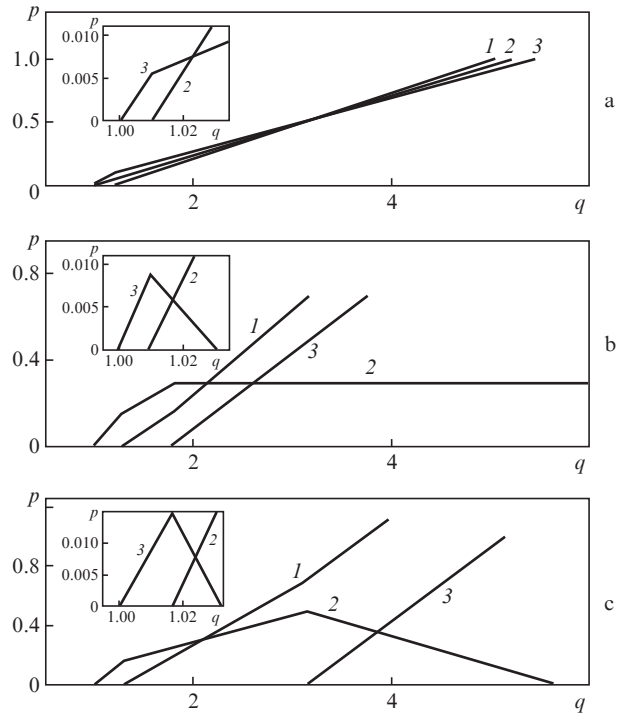

Figure 4. Output power as a function of parameter q for the (*1*) first, fifth, (*2*) second, fourth and (*3*) third channels in a five-channel laser at H = (a) 1, (b) 1.66 and (c) 2.1.

At low channel densities (Fig. 4a), their mutual effect is weak, so the channel powers differ rather little over the entire range of pump powers examined. At the same time, it is seen that, when threshold is reached in the first channel at $q = 1.2$, η_2 drops sharply. At the given additional losses, the channels have identical powers at $q = 3$.

At an increased channel density (Fig. 4b), after termination of lasing in the central channel in the range $1.04 < q < 1.27$, two-channel lasing in the even channels occurs. With increasing pump power, after threshold is reached in the first and fifth channels at $q = 1.27$, $\eta_{2,4}$ decreases. As a result of further increase in pump power, threshold is again reached in the central channel at $q = 1.8$, following which five-channel lasing occurs. A distinctive feature of the laser with an H value adjusted to the case under consideration is that its even channels lose sensitivity to changes in pump power ($\eta_{2,4} = 0$).

There is another noteworthy feature at an increased channel density: raising the pump power leads to termination of lasing in the even channels. In Fig. 4c, the lasing threshold in the central channel is reached at $q = 3.25$ and, at $q = 5.65$, lasing completely stops in the second and fourth channels. Thus, at a sufficient channel density and low pump power, two-channel lasing is possible. Increasing the pump power leads to four- and five-channel lasing. At high pump powers, there is three-channel lasing.

Figure 5 shows the five-channel lasing spectrum obtained experimentally at a low channel density ($\Delta\nu = 1$ ТГц, $H = 0.45$) and a pump current I_p = 170 mA. The central channel frequency is 194 THz. By adjusting additional losses in the channels (except in the central one), the powers in the five channels can be equalised with an accuracy of ~1 dB.

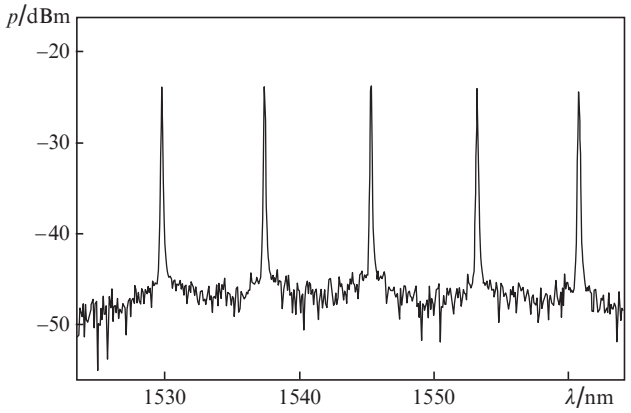

Figure 5. Five-channel lasing spectrum at a low channel density.

Comparison demonstrates that theoretical predictions and experimental data for the five-channel laser are in qualitative agreement: at a high channel density ($H = 2.1$), increasing the pump power leads to termination of lasing in the even channels and a transition to three-channel lasing. There is also agreement between the calculated and experimentally determined total output powers as functions of parameter q at different channel densities (Fig. 6).

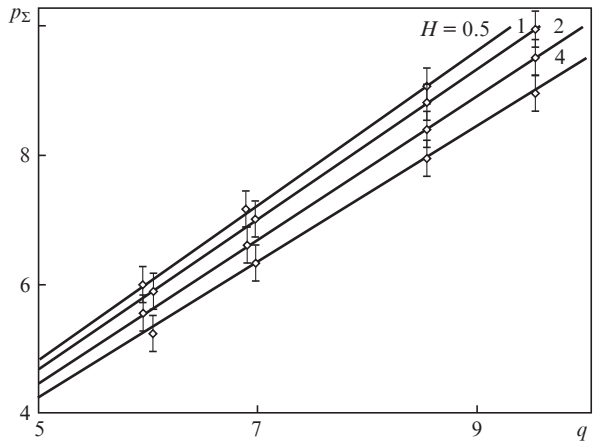

Figure 6. Calculated (solid lines) and measured (data points) total output powers as functions of parameter q for the five-channel laser at different H values.

4.3. Nine-channel laser

As the number of channels increases, the steady-state channel powers become rather difficult to equalise at high channel density ($H > 1.5$). Our calculations indicate that variations in losses introduced into individual channels cause power oscillations in all the channels, which decay with an extremely small increment. Figure 7 shows a stage of the transient process with $\tau \geqslant 1 \times 10^5$ (time dependences of output power for the first five channels). The total transient time is $\tau \approx 3 \times 10^5$ (real time of about 3 s). The powers of the other four channels, symmetric with respect to the fifth channel, approach those presented in Fig. 7 but are not identical to them. The curve representing the variation of the power in each channel slightly resembles a sinusoid. Oscillations in neighbouring channels are in antiphase, as would be expected.

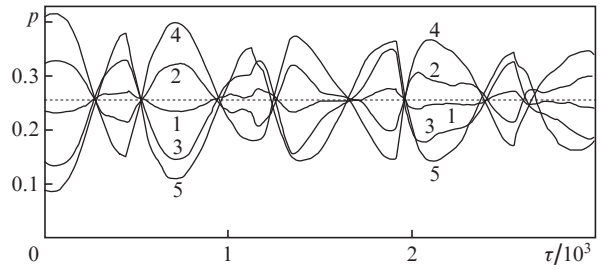

Figure 7. Power dynamics in the first five channels of the nine-channel laser ($q = 3$, $H = 1.8$). The curves are numbered according to the number of the channel. The dashed line represents the calculated steady-state power, which is the same for all the channels.

Experiments cannot be free of noise, which causes low-frequency power oscillations. For this reason, lasing with roughly equal powers of nine channels is possible at a still lower channel density. Figure 8 shows the experimentally measured lasing spectrum at $\Delta\nu = 500$ GHz ($H = 0.9$) and a pump current $I_p = 250$ mA. The additional loss produced in each channel by an attenuator is varied in 0.1-dB increments. We failed to stabilise channel powers in our experiments: there were pulsations up to 7 dB (standard deviation no greater than 3.2 dBm).

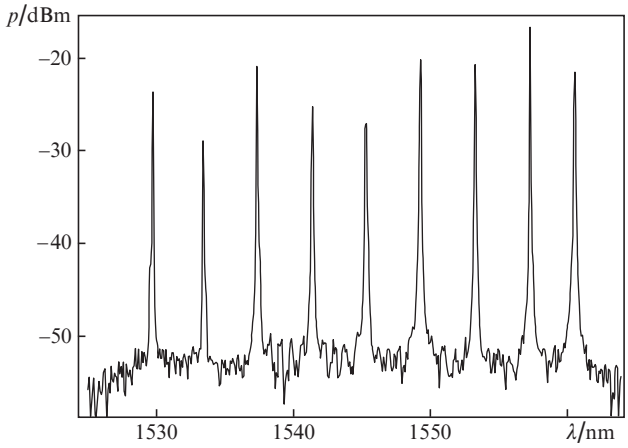

Figure 8. Power instability in nine channels (experimental data).

Lasing instability at a high channel density or a large number of channels limits the field of potential practical applications for nine-channel lasers. The limitation can be eliminated by using active instrumental channel power stabilisation, which will allow not only to drastically reduce the transient time but also to eliminate low-frequency parasitic fluctuations.

Figure 9 shows a schematic of a multichannel laser with an active instrumental channel power stabilisation. Its operating principle is as follows: Some of the laser output is demultiplexed after a 1/99 coupler and directed to a control system. At its input, photodetectors produce signals proportional to the powers of the corresponding channels. The signals are compared to the corresponding control voltages generated by the control system according to the required channel power as set by the user. The control system generates an error signal proportional to the difference between the power measured in the channel and that set by the system itself. The error signal is fed to a controlled attenuator, which introduces an additional loss proportional to the error signal, thereby closing the negative feedback loop, which ensures stabilisation of the predetermined output powers of the channels.

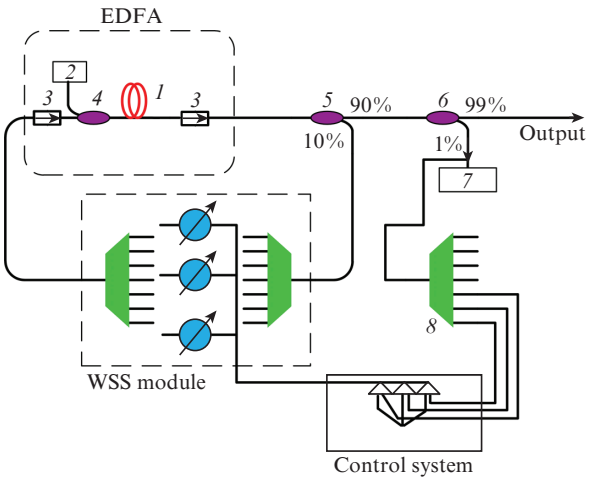

Figure 9. Schematic of a multichannel laser with an active instrumental channel power stabilisation:
(*1*) active element; (*2*) pump laser; (*3*) optical isolators; (*4*) wavelength-selective coupler; (*5*) 10/90 coupler; (*6*) 1/99 coupler; (*7*) spectrum analyser; (*8*) demultiplexer.

5. Conclusions

It has been shown that lasing characteristics of multichannel erbium-doped fibre lasers calculated in a model that uses spectrally dependent cross-saturation coefficients of the channels agree with experimental data.

It has been demonstrated experimentally that the competition between the channels in a multichannel erbium-doped fibre laser increases markedly when the channel frequency spacing is less than the full width at half maximum of the spectral dip in the gain profile (about 450 GHz). The increased competition between the channels makes it impossible to achieve high stability of lasing at a large number of channels.

It has been shown theoretically and experimentally that, in lasers having nine or more channels, perturbations arising from loss variations have so small damping increments that power oscillations persist for several seconds in real time. As a result, even weak low-frequency noise in experiments is capable of 'feeding' such oscillations. The use of active channel power stabilisation will allow to make lasers with a number of channels necessary for testing telecommunication links.

References

1. Zhang C., Zhao J.F., Miao C.Y. *Laser Phys.*, **22**, 1573 (2012).
2. Basov N.G. et al. *Kvantovaya Elektron.*, **11**, 1084 (1984) [*Sov. J. Quantum Electron.*, **14**, 731 (1984)].
3. Kravtsov N.V., Nanii O.E., Shabat'ko N.V. *Kvantovaya Elektron.*, **19**, 994 (1992) [*Sov. J. Quantum Electron.*, **22**, 925 (1992)].
4. Nanii O.E. et al. *Laser Phys.*, **18**, 1238 (2008).
5. Jiao M.-X. et al. *J. Phys. Conf. Ser.*, **48**, 1482 (2007).
6. Yao J.P. *J. Lightwave Technol.*, **27**, 314 (2009).
7. Nanii O.E. *Kvantovaya Elektron.*, **19**, 762 (1992) [*Sov. J. Quantum Electron.*, **22**, 703 (1992)].
8. Hu Z.L., Xu P., Jiang N. *Laser Phys.*, **22**, 1590 (2012).
9. Kir'yanov A.V. et al. *Vestn. Mosk. Univ.*, (1), 81 (1986) [*Moscow Univ. Phys. Bull.*, **41** (1), 93 (1986)].
10. Nanii O.E., Shelaev A.N. *Kvantovaya Elektron.*, **16**, 1122 (1989) [*Sov. J. Quantum Electron.*, **19**, 726 (1989)].
11. Schwartz S., Gutty F., Feugnet G., Loil É., Pocholle J. *Opt. Lett.*, **34**, 3884 (2009).
12. McKay A., Dawes J.M., Park J.D. *Opt. Express*, **15**, 16342 (2007).
13. Zelenin D.V. et al. *Kvantovaya Elektron.*, **32**, 5 (2002) [*Quantum Electron.*, **32**, 5 (2002)].
14. Gurkin N.V. et al. *Laser Phys. Lett.*, **11**, 095103 (2014).
15. Yushko O.V. et al. *Kvantovaya Elektron.*, **45**, 75 (2015) [*Quantum Electron.*, **45**, 75 (2015)].
16. Redyuk A.A. et al. *Laser Phys. Lett.*, **12**, 025101 (2015).
17. Gainov V.V. et al. *Laser Phys. Lett.*, **10**, 075107 (2013).
18. Gurkin N.V. et al. *Kvantovaya Elektron.*, **43**, 546 (2013) [*Quantum Electron.*, **43**, 546 (2013)].
19. Konyshev V.A. et al. *Opt. Commun.*, **349**, 19 (2015).
20. Konyshev V.A. et al. *Opt. Commun.*, **355**, 279 (2015).
21. Redyuk A.A. et al. *Laser Phys. Lett.*, **12**, 025101 (2015).
22. Gainov V.V. et al. *Zh. Tekh. Fiz.*, **85**, 83 (2015) [*Tech. Phys.*, **60** (4), 561 (2015)].
23. Popov D.A. et al., *Vestn. Mosk. Univ.*, (5) 62 (2015) [*Moscow Univ. Phys. Bull.*, **70** (5), 390 (2015)].
24. Park N., Wysocki P.F. *Photonics Technol. Lett.*, **8**, 1459 (1996).
25. Chen D., Qin S., He S. *Opt. Express*, **15**, 930 (2007).
26. Zhan L. et al. *Opt. Express*, **14**, 10233 (2006).
27. Chen Z., Ma S., Dutta N.K. *Opt. Express*, **17**, 1234 (2009).
28. Zhang Z.X. et al. *Opt. Lett.*, **33**, 324 (2008).
29. Feng X.H., Tam H.Y., Wai P.K.A. *Opt. Express*, **14**, 8205 (2006).
30. Feng X.H. et al. *Opt. Commun.*, **268**, 278 (2006).
31. Liu X. et al. *Opt. Express*, **20**, 7088 (2012).
32. Nanii O.E. *Kvantovaya Elektron.*, **23**, 17 (1996) [*Quantum Electron.*, **26**, 15 (1996)].
33. Bolshtyansky M. *J. Lightwave Technol.*, **21**, 1032 (2003).